AUT Journal of Mechanical Engineering

AUT J. Mech. Eng., 6(3) (2022) 427-442
DOI: 10.22060/ajme.2022.20632.6012

Evaluation of Micropolar Fluid Transport through Penetrable Medium: Effect of Flow and Thermal Slip

A. T. Akinshilo[1*], M. G. Sobamowo[1], A. Adingwupu[2]

[1] Department of Mechanical Engineering, University of Lagos, Akoka-Yaba, Nigeria
[2] Department of Mechanical Engineering, Igbinedion University, Edo, Nigeria

ABSTRACT: In this study, the micropolar fluid flow through penetrable walls under slip flow and thermal jump condition is examined. The Micropolar fluid accounts for the hydrodynamic limit of the classical Navier Stokes model, it takes into consideration the micro-structure of the fluid, local structure, and micro rotation of fluid particles. Here the thermal exchange and mass transport of the micropolar fluid are studied considering transport conditions such as radiation, variable magnetism, and nanoparticle concentration. The micropolar fluid flows into the channel and exits under slip velocity and temperature jump condition. The channel walls are assumed porous, fluid is incompressible, Newtonian, and flowing steadily. The mechanics of the fluid is described by coupled, highly successive, nonlinear system of higher-order partial differential equations transformed using appropriate similarity transform to ordinary differentials. These are analyzed by adopting the Homotopy perturbation method of analysis. Results obtained from the analysis show a quantitative increase of nanoparticle concentration from enhanced thermal transfer, which effect is significant towards the lower plate. Similarly, radiation increase reveals higher heat transfer while the Reynolds parameter shows reducing heat transfer. Results obtained compared with similar literature are in good agreement. The study finds good application in tribology, ferrofluids, and arterial blood flow amongst other practical, yet relevant applications.

Review History:

Received: Oct. 05, 2021
Revised: Jan. 07, 2022
Accepted: Feb. 16, 2022
Available Online: Apr. 28, 2022

Keywords:

Micropolar fluids
Thermal radiation
Slip flow
Thermal jump
Homotopy perturbation method.

1- Introduction

The study of Micropolar fluid transport phenomena over the years cannot be over-emphasized. As the Micropolar fluid accounts for the hydrodynamic limit of the classical Navier Stokes model, this fluid takes into consideration the micro-structure of the fluid, local structure, and micro rotation of fluid particles. The model proposed by Eringen [1] to study the effect of this fluid can be explained by considering the micro-rotation effect of fluid particles during flow. Similarly, the study of micropolar heat transfer and flow through porous plates was studied by Aurangzaib et al. [2]. The transport of micropolar fluid was studied by Bank and Dash [3] through a porous medium with the impact of the magnetic field. Sheikholelami et al. [4] analyzed the micropolar fluid flow through a porous medium with the aid of analytical methods. The pulsatile flow of magneto micropolar fluid on peristaltic motion through a porous medium was investigated by Mekhar and Mohammed [5]. Viscous dissipation of micropolar fluid flowing past a stretching plate nonlinearly was investigated by Ahmad et al. [6]. Magnetic intensity influence on micropolar fluid was studied by Deo et al. [7] using a cylindrical tube with an impermeable core. Newtonian and non-Newtonian analysis of flow was performed by Hatami and Jing [7] using semi-analytical analysis. Micropolar magneto hydrodynamic convective flow due to deformable porous heated plate was studied by Trkyilmazoglu [8]. Flow and heat transfer was examined by Akinshilo [9] for injection nanofluid flow through expanding and contracting porous channel. Viscous dissipation and joule heating effect are investigated on the micropolar fluid flow by Lund et al. [10] flowing over a shrinking sheet. Heat and mass flow of micropolar fluid was analyzed using computational analysis by Ahmad et al. [11]. The combined effect of absorption and heat generation on micropolar fluid under chemical reaction was presented by Damseh et al. [12] flowing over stretched permeable surface uniformly. Micropolar flow with nanoparticles was presented by Alizadeh et al. [13] under the influence of thermal radiation and a constant magnetic field. The effect of heat flux applied uniformly and heat generation on micropolar fluid flowing vertically along a permeable plate was studied by Rahman et al. [14]. Nanofluid flows through parallel plates embedded with the porous medium were studied by Akinshilo [15].

The importance of the nanoparticles during heat transfer cannot be overemphasized as it raises fluid thermal conductivity, consequently saving energy. This has stimulated the researcher's interest in the application of nanoparticles to fluid heat transfer. Hence water-based Single-Walled Carbon Nanotubes (SWCNTs) and Multi-Walled Carbon Nanotubes (MWCNTs) particles' non-Darcy flow was studied by Hayat et al. [16] having multiple slips. Intermolecular adhesive and cohesive forces sensitivity of MWCNTs incorporated into

*Corresponding author's email: ta.akinshilo@gmail.com

paraffin was presented by Yan et al. [17]. Tian et al. [18] studied the rheological behavior of hybrid MWCNTs and copper oxide nanofluid in a suspension of water and ethylene glycol. Pulsatile blood flow motion was modeled in the elastic artery by Sharifzadeh et al. [19] for biomedical applications. The dynamics of molecules on ferro nanofluid considering barrier effects were analyzed by Fazinpour et al. [20] in the presence of an external, time-dependent magnetic field. Yan et al. [21] investigated the rheological properties of hybrid MWCNTs and TiO_2 nanofluid. Type of nanoparticle, base temperature, size, and shape was studied on the convective boundary layer of nanofluid by Zakari et al. [22]. Thermal and mass transfer effect on convective boundary layer was studied by Refs. [23-26] through transport medium.

Since problems of these types are usually nonlinear in nature, which demands boundary value coupled system higher-order models. Analyzing, investigating and examination of the mechanics of the micropolar flow transport and thermal transfer requires either numerical or analytical methods as suitable methods of analysis utilized by researchers over the years [27-49]. These methods of analysis include the Akbari-Ganji Method (AGM), Differential Transform Method (DTM), method of weighted residuals (Garlerkins, collocation, and least squares), Adomian Decomposition Method (ADM), Homotopy Analysis Methods (HAM) and Variation Of Iteration Method (VIM) amongst others. The AGM is an iterative method that is time-consuming for systems of strongly nonlinear models, the errors of approximation due to iteration is low. Computation stencils are required for the analysis of HAM in the determination of its initial or guess term, auxiliary function, and parameter. This results in large computational cost, the HAM as the ability to solve complex ordinary or partial systems of equations. VIM and the method of weighted residuals suffer from errors of approximation but the method of analysis is relatively simple. The DTM requires the use of programmable tools such as Matlab or Maple in handling strongly nonlinear analysis. The analysis of ADM involves solving Adomian polynomials which are rigorous for nonlinear equations. The Homotopy Perturbation Method (HPM) is selected in this study as the preferred analytical scheme to analyze the problem. This is owing to a rapid rate of convergence of approximate analytical solutions, accuracy, and reliability of data obtained from the investigation of the coupled system of nonlinear mechanics governing mass and heat transfer.

With respect to the above, this study investigates the effect of velocity slip and thermal jump on the steady micropolar fluid transport through the penetrable medium. The system of mechanics of fluid transport is described by nonlinear models and analyzed using the Homotopy perturbation method with obtained solutions validated against the Fourth order Runge Kutta Fehlberg numerical method. This proves to be in excellent agreement, increasing confidence in obtained results.

2- Problem Description and Governing Equations

The two dimension micropolar steady flow in a horizontal channel is considered in this section. The micropolar fluid flows into the channel and exits under slip velocity and temperature jump condition. As described in Fig. 1, the bottom wall is defined as T_1 , and the top wall temperature is indicated as T_2 . The channel walls are assumed porous, fluid is incompressible, Newtonian, and flowing steadily. The parallel surface to the channel wall is the x axis and normal to the wall is the y axis. The walls of the channels are located at $y = \pm h$. A thermal equilibrium condition is assumed between the base fluid and nanoparticles. Velocity slip and thermal jump influence on flowing micropolar fluid particles under constantly applied magnetic field is considered. Subject to the above illustrations, governing equations for momentum and energy are presented as follows [13]:

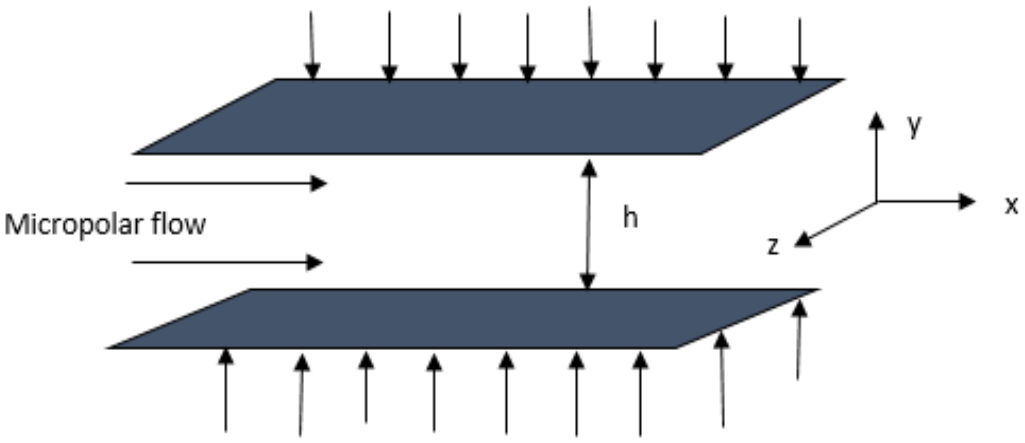

Fig. 1. Physical model of the problem.

$$\frac{\partial u}{\partial x}+\frac{\partial v}{\partial y}=0 \tag{1}$$

$$\rho_{nf}\left(u\frac{\partial u}{\partial x}+v\frac{\partial u}{\partial y}\right)=-\frac{\partial p}{\partial x}+ \left(\mu_{nf}+k\right)\left(\frac{\partial^2 u}{\partial x^2}+\frac{\partial^2 u}{\partial y^2}\right)+k\frac{\partial N}{\partial y}-\sigma_f B_0^2 u \tag{2}$$

$$\rho_{nf}\left(u\frac{\partial v}{\partial x}+v\frac{\partial v}{\partial y}\right)=-\frac{\partial p}{\partial y}+ \left(\mu_{nf}+k\right)\left(\frac{\partial^2 v}{\partial x^2}+\frac{\partial^2 v}{\partial y^2}\right)-k\frac{\partial N}{\partial x} \tag{3}$$

$$\rho_{nf} j\left(u\frac{\partial N}{\partial x}+v\frac{\partial N}{\partial y}\right)= -k\left(2N+\frac{\partial u}{\partial y}-\frac{\partial v}{\partial x}\right)+\gamma_{nf}\left(\frac{\partial^2 N}{\partial x^2}+\frac{\partial^2 N}{\partial y^2}\right) \tag{4}$$

$$u\frac{\partial T}{\partial x}+v\frac{\partial T}{\partial y}= \frac{k_{nf}}{\left(\rho C_p\right)_{nf}}\left(\frac{\partial^2 T}{\partial x^2}+\frac{\partial^2 T}{\partial y^2}\right)-\frac{1}{\left(\rho C_p\right)_{nf}}\frac{\partial q_{rad.}}{\partial y} \tag{5}$$

Where the vortex viscosity is given as k, viscosity spin gradient is $\gamma nf=\left(\mu nf+k/2\right)j$, directional velocities in x and y direction are u and v respectively, Pressure is P, Temperature is T, the magnetic field is B_o, Micro rotation velocity is N, micro-inertia density is j and q_{rad} is the heat flux radiation and σf is the electrical fluid conductivity.

The Rooseland approximation for radiation is defined as Eqs. [50-51]

$$q_{rad.}=-\left(4\sigma^*/3k_{nf}^*\right)\frac{\partial T^4}{\partial y}. \tag{6}$$

Here the constant of Stefan Boltzmann is given as σ^* and the nanofluid mean absorption coefficient is k_{nf}^*. It is further assumed that the temperature difference within a flow is such that the Taylor series may expand T^4. Simplifying the terms, we obtain

$$T^4\cong 4T_\infty^3 T-3T_\infty^4. \tag{7}$$

Therefore, Eq. (5) is reduced to:

$$u\frac{\partial T}{\partial x}+v\frac{\partial T}{\partial y}=\frac{k_{nf}}{\left(\rho C_p\right)_{nf}}\left(\frac{\partial^2 T}{\partial x^2}+\frac{\partial^2 T}{\partial y^2}\right)+ \frac{16\sigma^* T_\infty^3}{3k_{nf}^*\left(\rho C_p\right)_{nf}}\frac{\partial^2 T}{\partial y^2} \tag{8}$$

The effective fluid viscosity of the nanofluid is μnf, nanofluid effective density is ρnf, nanofluid heat capacity is $\left(\rho nf\right)_{nf}$ and the nanofluid thermal conductivity is knf are given as:

$$\begin{aligned}&\rho_{nf}=\left(1-\phi\right)\rho_f+\phi\rho_s,\\ &\left(\rho C_p\right)_{nf}=\left(1-\phi\right)\left(\rho C_p\right)_f+\phi\left(\rho C_p\right)_s,\\ &\mu_{nf}=\frac{\mu_f}{\left(1-\phi\right)^{2.5}},\\ &\frac{k_{nf}}{k_f}=\frac{k_s+2k_f-2\phi\left(k_f-k_s\right)}{k_s+2k_f+2\phi\left(k_f-k_s\right)}.\end{aligned} \tag{9}$$

With appropriate boundary conditions given as:

$$\begin{aligned}&u=\beta_1\frac{\partial u}{\partial y} \quad v=0 \quad N=-s\frac{\partial u}{\partial y}\Big|_{y=0}\\ &T=\gamma_1\frac{\partial T}{\partial y}+T_0 \quad \text{At} \quad y=0,\\ &u=-\beta_1\frac{\partial u}{\partial y} \quad v=v_0, \quad N=-s\frac{\partial u}{\partial y}\Big|_{y=h}\\ &T=-\gamma_1\frac{\partial T}{\partial y}+T_h \quad \text{At} \quad y=+h.\end{aligned} \tag{10}$$

Here injection flows occur at $V_0<0$ and suction flows occur at $V_0>0$. The velocity slip is represented as β_1 and the thermal slip is denoted as γ_1. The rotational degree of the microelements near the walls and boundary parameter is s. For non-rotation close to the boundary wall, s=0. This condition corresponds to concentrated particle flows. Other similar cases have been considered by researchers such as $s=0.5$ and $s=1$. These connote weak and turbulent flow conditions respectively. The nondimensionalized parameters are introduced as:

$$\begin{aligned}&\eta=\frac{y}{h}, \quad u=-\frac{v_0 x}{h}f'(\eta), \quad N=\frac{v_0 x}{h^2}g(\eta),\\ &v=v_0 f(\eta), \quad \theta=\left(T-T_1\right)/\left(T_2-T_1\right).\end{aligned} \tag{11}$$

Given $T_2=T_1+Ax$, where A is a constant.

By substituting T_2 into the governing model of equations and pressure gradient is eliminated. Eqs. (2) to (4) and (8) are transformed into the following system of coupled nonlinear equations:

Table 1. Thermophysical properties of nanofluid Alizadeh et. al. [13].

	$\rho\left(\mathrm{kg/m^3}\right)$	$C_p\left(\mathrm{J/kgK}\right)$	$K\left(\mathrm{W/mK}\right)$
Copper (Cu)	8933	385	401
Water	997.1	4179	0.613

$$\left(1+(1-\phi)^{2.5}K\right)f^{iv}-(1-\phi)^{2.5}Kg''-\left(1-\phi+\frac{\rho_s}{\rho_f}\phi\right)(1-\phi)^{2.5}\mathrm{Re}\left(ff'''-ff''\right)-(1-\phi)^{2.5}Mf''=0 \tag{12}$$

$$\left(1+\frac{(1-\phi)^{2.5}}{2}K\right)g''+(1-\phi)^{2.5}K\left(f''-2g\right)-\left(1-\phi+\frac{\rho_s}{\rho_f}\phi\right)(1-\phi)^{2.5}\mathrm{Re}\left(fg'-gf'\right)=0 \tag{13}$$

$$\theta''+\left((1-\phi)+\frac{(\rho C_p)_s}{(\rho C_p)_f}\phi\right)\left(\frac{3}{3+4N}\right)\times\frac{k_f}{k_{nf}}\mathrm{Pr}\,\mathrm{Re}\left(f'\theta-f\theta'\right)=0 \tag{14}$$

Adopting the relevant boundary conditions

$$\begin{aligned}&f(0)=0,\quad f'(0)=\beta f'',\\ &f'(1)=-\beta f'',\quad f(1)=1,\\ &g(0)=0,\quad g(1)=0,\\ &\theta(0)=1+\gamma\theta',\quad \theta(1)=-\gamma\theta'.\end{aligned} \tag{15}$$

Where Reynold parameter is Re given $Re<0$ corresponds to injection flows while $Re>0$ corresponds to suction flows, the magnetic parameter is M, the micropolar parameter is given as K, and radiation parameter is N. These parameters are defined as follows:

$$\begin{aligned}&\mathrm{Re}=\rho_f v_0 h/\mu_f,\\ &\mathrm{Pr}=\mu_f C_{p,f}/k_f,\\ &N=4\sigma^* T_\infty^3/k_{nf}k_{nf}^*,\\ &M=\sigma_f B_0^2 h^2/\mu_f,\\ &K=k/\mu_f,\\ &j=h^2.\end{aligned} \tag{16}$$

Other important engineering parameters of interest is the Nusselt number which is specified as follows:

$$Nu^*=-\left(\frac{h}{k_f\left(T_2-T_1\right)}\right)\left(k_{nf}+\frac{16\sigma^* T_\infty^3}{3k_{nf}^*}\right)\left.\frac{\partial T}{\partial y}\right|_{y=-h} \tag{17}$$

In terms of (9) and (11), we gain:

$$Nu=\left|\frac{k_{nf}}{k_f}\left(1+\frac{4}{3}N\right)\theta'(-1)\right| \tag{18}$$

2- 1- Application of the homotopy perturbation method

Here the micropolar fluid flow through penetrable walls under slip and thermal jump condition are examined. The micropolar fluid flows steadily considering the magnetic field and thermal transport. The mechanics of rotating particle flow is described using nonlinear coupled systems of higher order equations, these are analyzed utilizing the Homotopy Perturbation Method (HPM). Whose principles and fundamentals have been extensively discussed by Sobamowo and Akinshilo [45]. The HPM has been an analytical method with a fast rate of convergence, coupled with procedural stability is the selected method adopted to solve the system of a coupled nonlinear model of higher differential. Therefore, constructing the Homotopy of the governing equations Eqs. (12) to (14) are expressed as:

$$H_1(\mathrm{p},\eta)=(1-p)\left[\frac{d^4 f}{\partial\eta^4}\right]+p\left[\frac{d^4 f}{d\eta^4}-(1-\phi)^{2.5}K\frac{d^2 g}{d\eta^2}-\left(1-\phi+\frac{\rho s}{\rho f}\phi\right)(1-\phi)^{2.5}\mathrm{Re}\left(f\frac{d^3 f}{d\eta^3}-f\frac{d^2 f}{d\eta^2}\right)-(1-\phi)^{2.5}M^2\frac{d^2 f}{d\eta^2}\right]/\left(1+(1-\phi)^{2.5}K\right)=0 \tag{19}$$

$$H_2(p,\eta)=(1-p)\left[\frac{d^2 g}{d\eta^2}\right]+p\left[\frac{d^2 g}{d\eta^2}-(1-\phi)^{2.5}K\left(\frac{d^2 f}{d\eta^2}-2g\right)-\left(1-\phi+\frac{\rho s}{\rho f}\phi\right)(1-\phi)^{2.5}\mathrm{Re}\left(f\frac{dg}{d\eta}-g\frac{df}{d\eta}\right)\right]/\left(1+\frac{(1-\phi)^{2.5}}{2}K\right)=0 \tag{20}$$

$$H_2(p,\eta)=(1-p)\left[\frac{d^2\theta}{d\eta^2}\right]+ p\left[\begin{array}{l}\frac{d^2\theta}{d\eta^2}+\left(\left(1-\phi\right)+\frac{\left(\rho C_p\right)_s}{\left(\rho C_p\right)_f}\phi\right)\times \\ \left(\frac{3N}{3N+4}\right)\frac{k_f}{k_{nf}}\Pr\mathrm{Re}\left(\frac{df}{d\eta}\theta-f\,\frac{d\theta}{d\eta}\right)\end{array}\right]=0 \quad (21)$$

Selecting power series of velocity and temperature profiles yields

$$f=P^0f_0+P^1f_1+P^2f_2+..... \quad (22a)$$

$$g=P^0g_0+P^1g_1+P^2g_2+..... \quad (22b)$$

$$\theta=P^0\theta_0+P^1\theta_1+P^2\theta_2+..... \quad (22c)$$

Eq. (22a) is substituted into (19) and selected at the various order yields

$$p^0:\frac{d^4f_0}{d\eta^4} \quad (23)$$

$$p^1:\left[\begin{array}{l}\frac{d^4f_1}{d\eta^4}-(1-\phi)^{2.5}K\,\frac{d^2g_0}{d\eta^2}- \\ \left(1-\phi+\frac{\rho s}{\rho f}\phi\right)(1-\phi)^{2.5}\mathrm{Re}\left(f_0\frac{d^3f_0}{d\eta^3}-f_0\frac{d^2f_0}{d\eta^2}\right)- \\ (1-\phi)^{2.5}M^2\frac{d^2f_0}{d\eta^2}\end{array}\right]/\left(1+(1-\phi)^{2.5}K\right) \quad (24)$$

$$p^2:\left[\begin{array}{l}\frac{d^4f_2}{d\eta^4}-(1-\phi)^{2.5}K\,\frac{d^2g_1}{d\eta^2}- \\ \left(1-\phi+\frac{\rho s}{\rho f}\phi\right)(1-\phi)^{2.5}\mathrm{Re}f_0\frac{d^3f_1}{d\eta^3}+ \\ \left(1-\phi+\frac{\rho s}{\rho f}\phi\right)(1-\phi)^{2.5}\mathrm{Re}f_0\frac{d^2f_1}{d\eta^2}- \\ (1-\phi)^{2.5}M\,\frac{d^2f_1}{d\eta^2}\end{array}\right]/\left(1+(1-\phi)^{2.5}K\right) \quad (25)$$

Eq. (22b) is substituted into (20) and selected at the various order yields

$$p^0:\frac{d^2g}{d\eta^2} \quad (26)$$

$$p^1:\left[\begin{array}{l}\frac{d^2g_1}{d\eta^2}-(1-\phi)^{2.5}K\left(\frac{d^2f_0}{d\eta^2}-2g_0\right)- \\ \left(1-\phi+\frac{\rho s}{\rho f}\phi\right)(1-\phi)^{2.5}\mathrm{Re}\left(f_0\frac{dg_0}{d\eta}-g_0\frac{df_0}{d\eta}\right)\end{array}\right]/\left(1+\frac{(1-\phi)^{2.5}}{2}K\right) \quad (27)$$

$$p^2:\left[\begin{array}{l}\frac{\mathrm{d}^2g_2}{d\eta^2}+\left(1-\phi\right)^{2.5}K\,\frac{\mathrm{d}^2f_1}{d\eta^2}-2g_1- \\ \left(1-\phi+\frac{\rho s}{\rho f}\phi\right)(1-\phi)^{2.5}\mathrm{Re}f_0\frac{dg_1}{d\eta}+ \\ \left(1-\phi+\frac{\rho s}{\rho f}\phi\right)(1-\phi)^{2.5}\mathrm{Re}g_0\frac{df_1}{d\eta}\end{array}\right]/\left(1+\frac{(1-\phi)^{2.5}}{2}K\right) \quad (28)$$

Eq. (22c) is substituted into (21) and selected at the various order yields

$$p^0:\frac{d^2\theta_0}{d\eta^2} \quad (29)$$

$$p^1:\frac{d^2\theta}{d\eta^2}+\left(\left(1-\phi\right)+\frac{\left(\rho C_p\right)_s}{\left(\rho C_p\right)_f}\phi\right)\left(\frac{3N}{3N+4}\right)\frac{k_f}{k_{nf}}\Pr\mathrm{Re}\left(\frac{df}{d\eta}\theta-f\frac{d\theta}{d\eta}\right) \quad (30)$$

$$p^2:\frac{\mathrm{d}^2\theta_2}{d\eta^2}+\left(\left(1-\phi\right)+\frac{\left(\rho C_p\right)_s}{\left(\rho C_p\right)_f}\phi\right)\left(\frac{3N}{3N+4}\right)\frac{k_f}{k_{nf}}\Pr\mathrm{Re}\left(\frac{df_0}{d\eta}\theta_1-f_0\frac{d\theta_1}{d\eta}\right) \quad (31)$$

Boundary condition for leading order is given as

$$f_0(0)=0\quad \frac{df_0}{d\eta}(0)=\beta\frac{df^2_0}{d\eta^2}\quad \frac{df_0}{d\eta}(1)=-\beta\frac{d^2f_0}{d\eta^2}\quad f_0(1)=1 \quad (32)$$

Solving Eq. (23) using the leading order boundary condition Eq. (32) yields

$$f_0 = \frac{2A\eta^3 - 3A\eta^2 + 6A\beta\eta}{6\beta - 1} \tag{33}$$

Boundary condition for leading order is given as

$$g_0(0) = 0, g_0(1) = 0 \tag{34}$$

Solving Eq. (26) using the leading order boundary condition Eq. (34) yields

$$g_0 = \frac{\eta + (\gamma - 1)}{2\gamma - 1} \tag{35}$$

Boundary condition for leading order is given as

$$\theta_0(0) = 1 + \gamma \frac{d\theta_0}{d\eta}, \theta_0(1) = -\gamma \frac{d\theta_0}{d\eta} \tag{36}$$

Solving Eq. (29) using the leading order boundary condition Eq. (36) yields

$$\theta_0 = 0 \tag{37}$$

Boundary condition for first order is given as

$$f_1(0) = 0 \quad \frac{df_1}{d\eta}(0) = \beta \frac{df^2_1}{d\eta^2} \quad \frac{df_1}{d\eta}(1) = -\beta \frac{d^2 f_1}{d\eta^2}$$
$$f_1(1) = 1 \tag{38}$$

Solving Eq. (24) using the first order boundary condition Eq. (38) yields

$$\begin{aligned} f_1 = {} & \eta^5(((9A^2\beta \operatorname{Re}\rho_f)/2 - \\ & (9A^2\beta \operatorname{Re}\rho_f\phi)/2 + 9A^2BRE\phi\rho_s)/ \\ & 2/(5\rho_f(6\beta-1)^2(K(1-\phi)^{2.5}+1)) - \\ & ((AM\rho_f(1-\phi)^{2.5} - 3A\beta M\rho_f(1-\phi)^{2.5}/ \\ & (5\rho_f(6\beta-1)^2(K(1-\phi)^{2.5}+1)(m+1))) + \\ & \eta^3((S(70A\rho_f - 840A\beta m\rho_f + \\ & 70AK\rho_f(1-\phi)^{2.5} - 840A\beta m\rho_f + \\ & 70AK\rho_f(1-\phi)^{2.5} + 7AM\rho_f(1-\phi)^{2.5} - \\ & 840A\beta K\rho_f(1-\phi)^{2.5} - 77A\beta M\rho_f(1-\phi)^{2.5} + \ldots \end{aligned} \tag{39}$$

Boundary condition for first order is given as

$$g_1(0) = 0, g_1(1) = 0 \tag{40}$$

Solving Eq. (27) using the first order boundary condition Eq. (40) yields

$$\begin{aligned} g_1 = {} & ((18\,\mathrm{ANPrRek}_f\rho_{cf} - 18AN\operatorname{PrRe}k_f\rho_{cf} + \\ & 18AN\operatorname{PrRe}k_f\rho_{cs}\phi)/ \\ & (4k_{nf}\rho_{cf}(6\beta-1)(3N+4)(4R+3)(2\gamma-1) - \\ & (18AN\operatorname{PrRe}k_f\rho_{cf} - 18AN\operatorname{PrRe}k_f\rho_{cf}\phi + \\ & 18AN\operatorname{PrRe}k_f\rho_{cs}\phi)/ \\ & (8k_{nf}\rho_{cs}\phi)/(8k_{nf}\rho_{cf}(6\beta-1)(3N+4)+(4R+3)))\eta^4 - \\ & ((9AN\operatorname{PrRe}k_f\rho_{cf} - 9AN\operatorname{PrRe}k_f\rho_{cf} + \ldots \end{aligned} \tag{41}$$

Boundary condition for first order is given as

$$\theta_1(0) = 1 + \gamma \frac{d\theta_1}{d\eta}, \theta_1(1) = -\gamma \frac{d\theta_1}{d\eta} \tag{42}$$

Solving Eq. (30) using the first order boundary condition Eq. (42) yields

$$\begin{aligned} \theta_1 = {} & -((12AK(12\beta-2)(1-\phi)^{2.5} - \\ & 12AK(K-6\beta K)(\phi-1)^5)\eta^3)/ \\ & (3(12\beta-2)^2 + 3(K-6\beta K) + \\ & ((12AK(12\beta-2)(1-\phi)^{2.5} - \\ & 12AK(K-6-\beta K)(\phi-1)^5)\eta^2)/ \\ & (2(12\beta-2)^2 + \ldots \end{aligned} \tag{43}$$

The Eqs (25), (28) and (31) second order solutions p^2 for $\mathrm{F}(\eta)$, $\mathrm{g}(\eta)$ and $\theta(\eta)$ were too voluminous. However they were represented in results validation and the graphical figures. Hence, expressions for final flow and heat transfer are given as:

$$\mathrm{f}(\eta) = f_0(\eta) + f_1(\eta) + f_2(\eta) \tag{44}$$

$$\mathrm{g}(\eta) = g_0(\eta) + g_1(\eta) + g_2(\eta) \tag{45}$$

$$(\eta) = \theta_0(\eta) + \theta_1(\eta) + \theta_2(\eta) \tag{46}$$

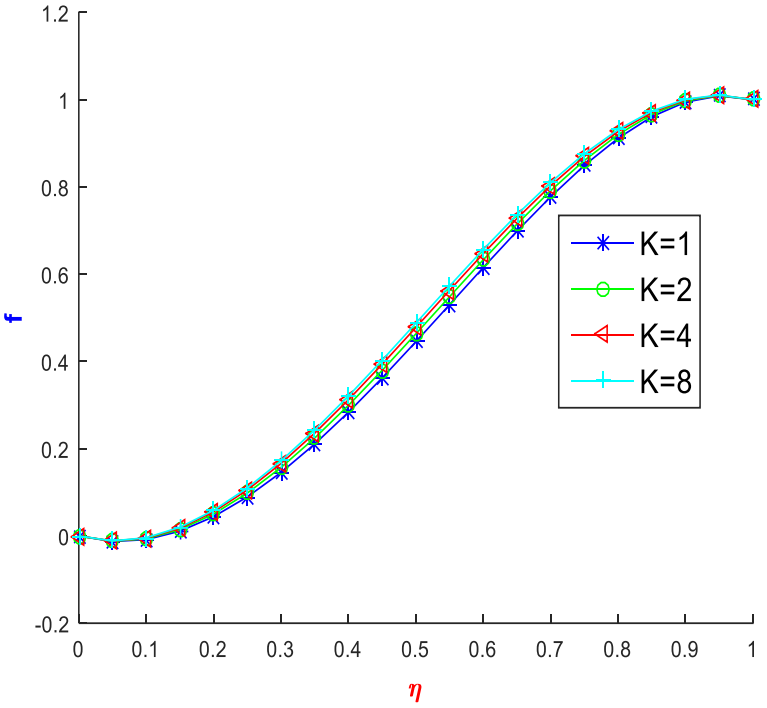

Fig. 2. Effects of the micro polar parameter (K) on velocity.

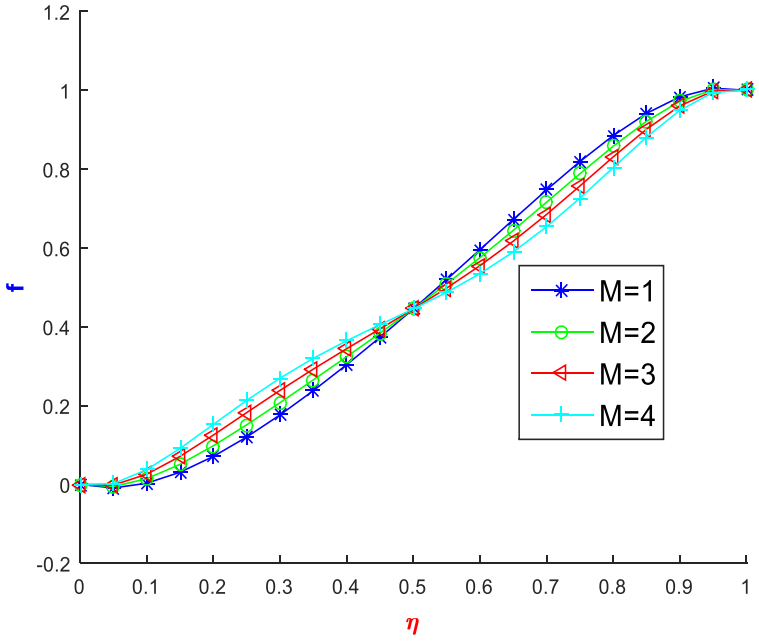

Fig. 3. Effects of the magnetic parameter (M) on velocity.

3- Results and Discussion

In this section, the result obtained from the analytical investigation of the coupled nonlinear higher order model for flow and thermal transport is reported graphically. At higher quantitative values of the Reynolds parameter for velocity, the fluid flow is impeded and thermal transfer is enhanced. In the same vein, no effect is noticed on the micro rotation profile. Fig. 2 reveals the effect of enhanced micropolar parameter on fluid transport through the penetrable medium, as observed this depicts a steady increase of fluid-particle velocity from the lower plate to the upper plate. This can be physically explained owing to decreasing momentum boundary layer thickness, as freely colliding rotating particles reduce kinematic viscosity. Also, the effect of micropolar fluid flow under constant magnetic field effect is seen in Fig. 3, this reveals applied magneto hydrodynamic influence on

fluid particle motion is enhanced until about the mid-plate $\eta = 0.5$ (not determined accurately) thereafter a reverse in flow trend towards the upper plate is seen. This phenomenon is a result of resistive force boundary forces known as Lorentz force towards channel boundary which limits fluid flow, consequently, the intensity of magnetic field abates.The thermal effect on the micropolar flow is observed in Figs. 4 to 6. As observed in Fig. 4 improving the Prandtl number effect is seen in the thermal distribution. As seen high Prandtl number increases thermal distribution along the flow medium as the thermal boundary layer improves due to the temperature gradient at the channel surface. The increasing effect of radiation is observed in Fig. 5, as the micropolar fluid flows through the channel, this reveals a high radiation abate temperature. Due to the rapid exchange of heat during the flow transport, hence improved heat transfer diminishes thermal

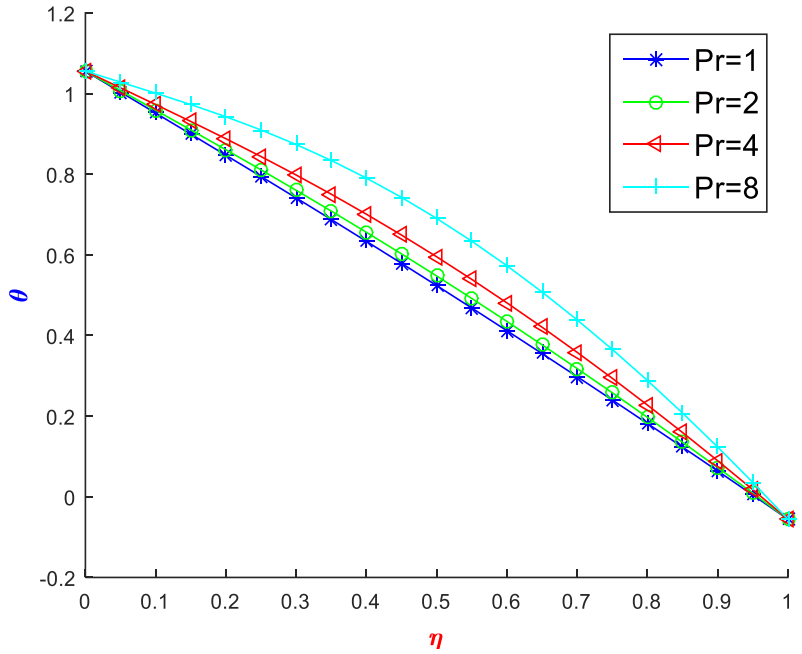

Fig. 4. Effects of Prandtl number (Pr) on temperature.

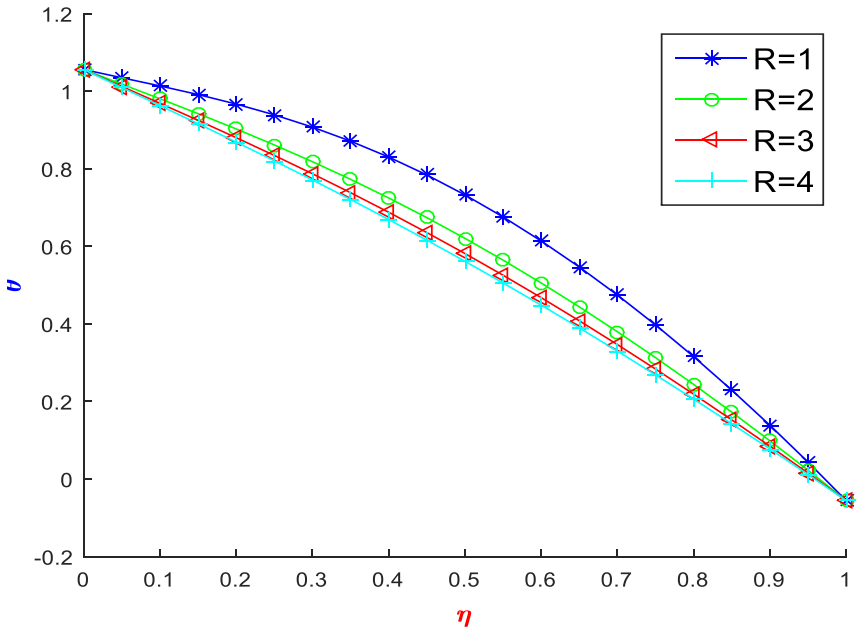

Fig. 5. Effects of Radiation parameter (R) on temperature.

layer thickness. The concentration of nanoparticle in a micropolar fluid is analyzed in Fig. 6. Increasing the concentration of nanoparticles of copper causes high energy exchange as the fluid flows reducing thermal boundary layer thickness for the micropolar nano mix. This improves heat transfer which is significant at the lower plate.The micro rotation effect of fluid molecules is represented in Figs 7 to 9. It is observed in Fig. 7, that micropolar parameter enhancement increases the rotation of fluid molecules from the lower to the upper plate. Rotation of fluid particles surges during fluid flow as

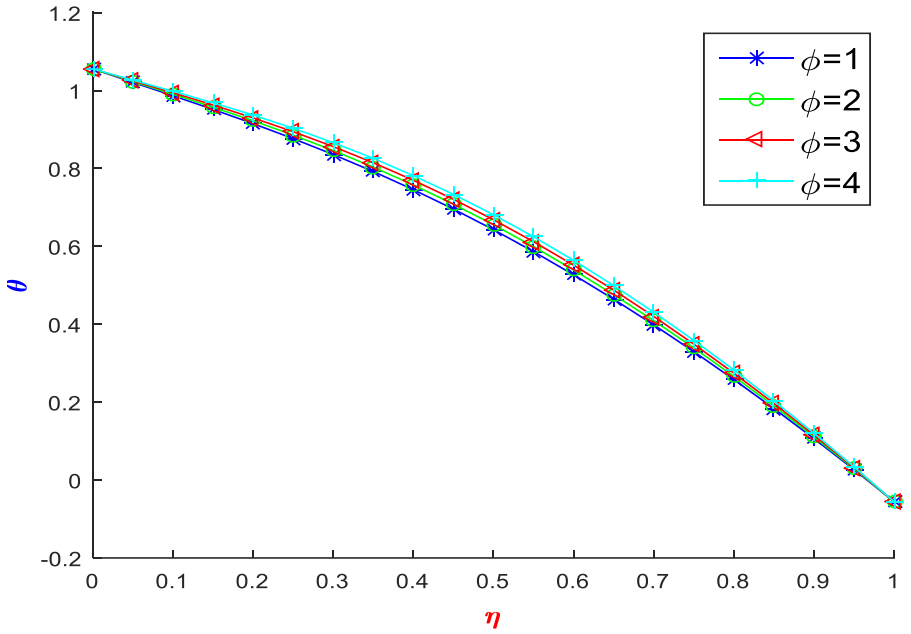

Fig. 6. Effects of nanoparticle concentration (ϕ) on temperature.

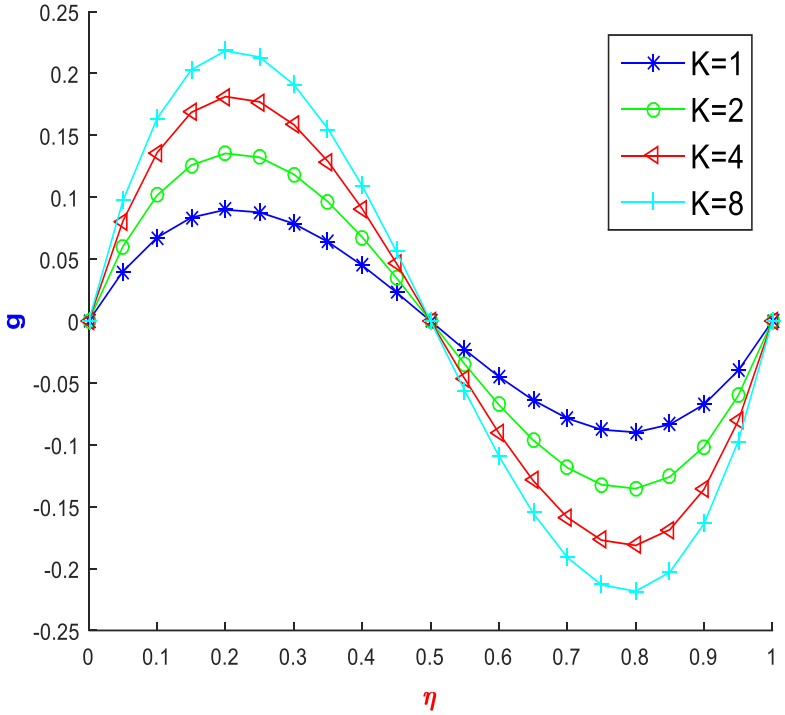

Fig. 7. Effects of micro polar (K) on rotation.

the colliding motion of fluid particles abates fluid viscosity owing to increased heat dissipation. However, molecules' rotation of micro particles is observed to abate in Fig. 8 as the concentration of nanoparticles increases from 1-8%. The temperature constant (A) effect on the micro flow rotation of rotating fluid particles is discussed in Fig. 9, this shows a surge in rotation of particles from the lower plate, however at mid plate decline of fluid rotation is observed till the upper plate. As a result of the thermal gradient effect at the channel boundary. Skin friction effect due to movement of micropolar

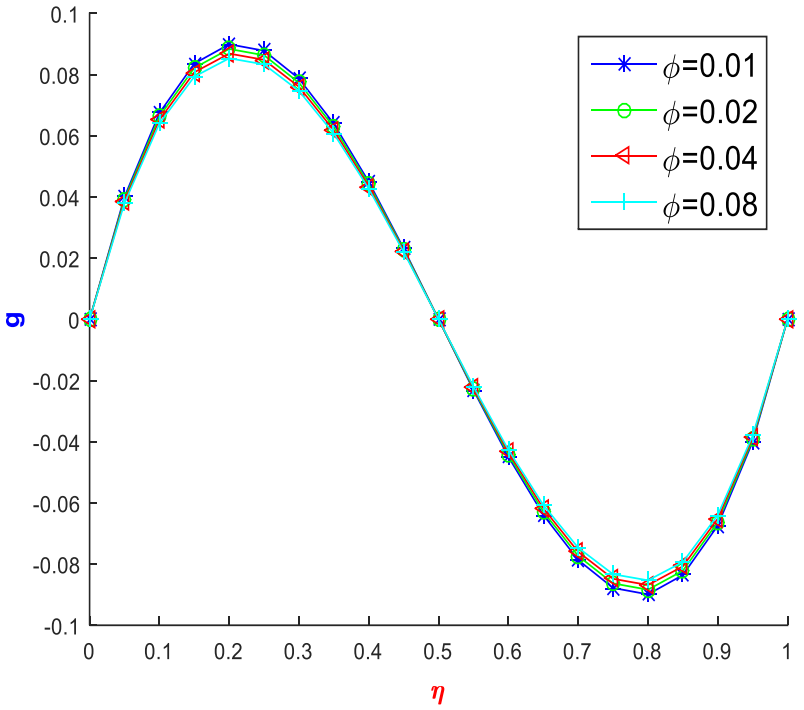

Fig. 8. Effects of nanoparticle concentration (ϕ) on rotation.

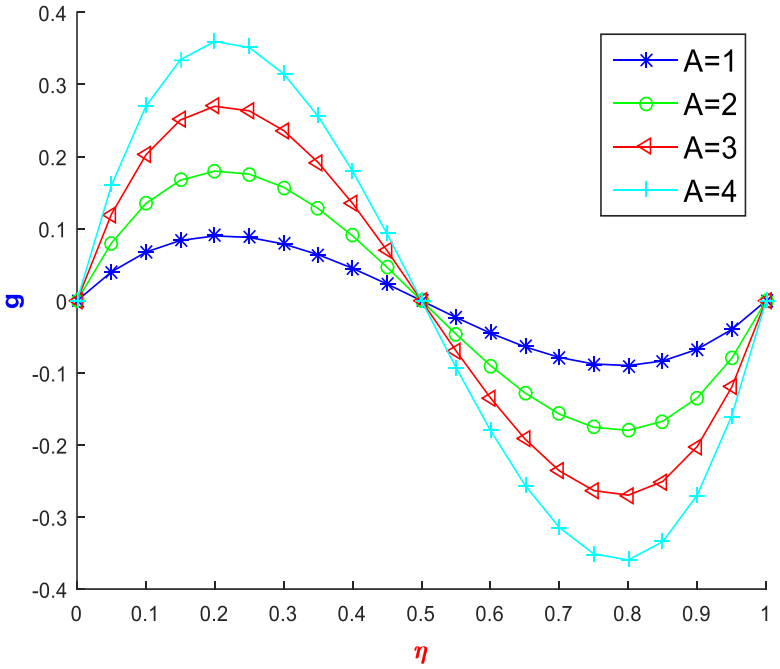

Fig. 9. Effects of A parameter on rotation.

fluid along the boundary is seen, this shows shear stress is enhanced by improving micropolar parameter. The effect of the Reynolds number is seen on the micropolar fluid flow, this reveals a decline in shear stress consequently improving flow from the lower plate up to the higher plate as shown in Fig. 10. Effect of the Prandtl number on the thermal transfer is seen in Fig. 11, as observed from the illustration Prandtl number abates the heat transfer process, though at a slight rate. Also, the Reynolds number drops as a viscous force on the micropolar fluid becomes more dominant. Radiation

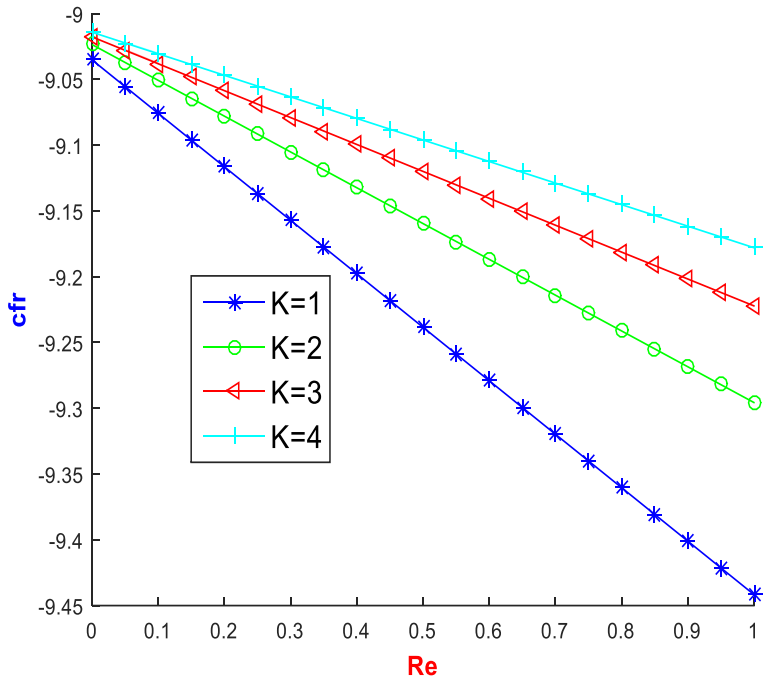

Fig. 10. Effects of Reynolds parameter (Re) and micro polar (K) on skin friction.

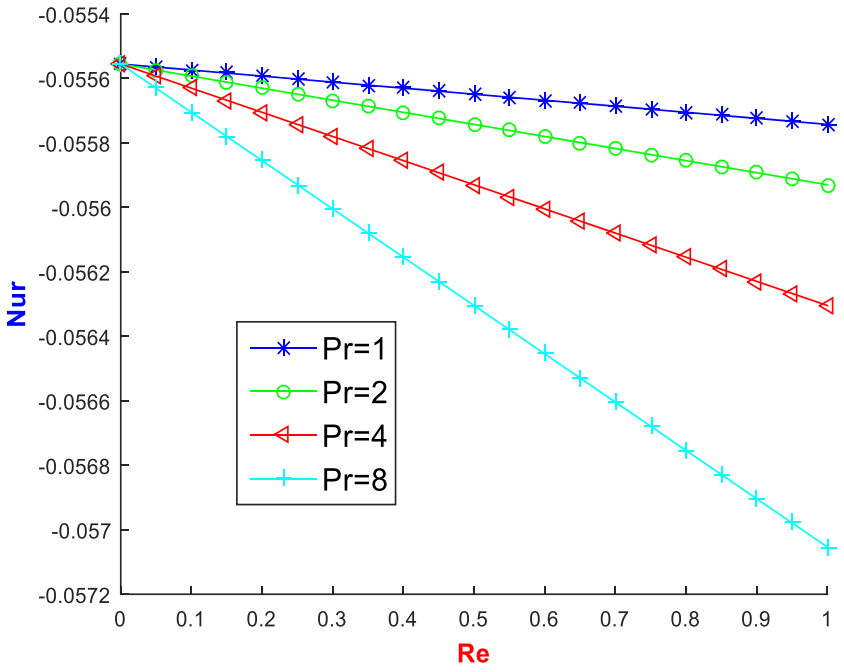

Fig. 11. Effects of Reynolds parameter (Re) and Prandtl number (Pr) on Nusselt number.

enhancement of the micropolar fluid molecules on thermal exchange is observed in Fig. 12, this shows noteworthy improvement in heat transfer. While the Reynolds effect on heat transfer reduces thermal exchange along the lower to the upper plate. Further, the validation of the results is expressed in Tables 2 to 4 compared against the fourth-order Runge Kutta Fehlberg method at constant parametric values of $Re = 5, M = 2, Da = 0.1, N = 1, Pr = 2, m = 1, A = 1, K = 1, = 0.01, == 0.05$, this proves a satisfactory conclusion. As observed in Table 2, fluid transport increases steadily across the transport medium from the lower to the upper plate. The thermal exchange of fluid particles and the relating boundary is seen in Table 3, this shows the temperature at the lower plate is higher and decreases significantly as the fluid particles approach the boundary of the lower plate surface. The rotation of micropolar fluid particles across the flow medium is expressed in Table 4, this reveals the particles move from the lower plate and reaches their peak at the mid-plate. Thereafter the fluid rotation falls as it approaches the upper plate.

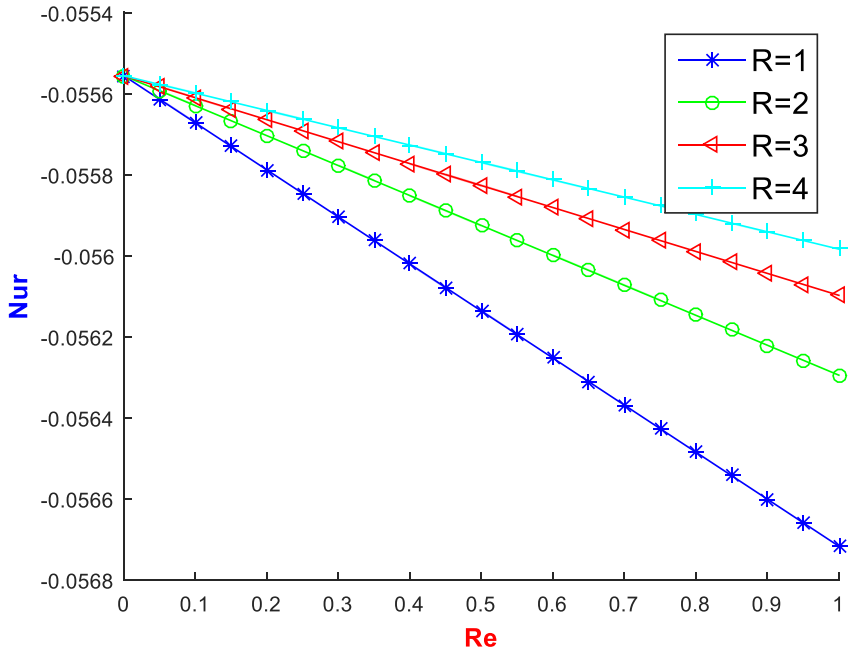

Fig. 12. Effects of Reynolds parameter (Re) and Radiation parameter (R) on Nusselt number.

Table 2. Comparison of various values of η for velocity profile.

η	RK-4 *@Re=5*	Present Work *@Re=5*	RK-4 *@Re=10*	Present Work *@Re=10*
0.0	0.0000	0.0000	0.0000	0.0000
0.1	-0.0083	-0.0083	-0.0140	-0.0140
0.2	0.0442	0.0442	0.0250	0.0250
0.3	0.1456	0.1456	0.1105	0.1105
0.4	0.2835	0.2835	0.2353	0.2353
0.5	0.4450	0.4450	0.3901	0.3901
0.6	0.6154	0.6154	0.5625	0.5625
0.7	0.7750	0.775	0.7356	0.7356
0.8	0.9116	0.9116	0.8865	0.8865
0.9	0.9945	0.9945	0.9864	0.9864
1.0	1.0000	1.0000	1.0000	1.0000

Table 3. Comparison of various values of η for temperature profile.

η	RK-4 *@Re=5*	Present Work *@Re=5*	RK-4 *@Re=10*	Present Work *@Re=10*
0.0	1.0556	1.0556	1.0556	1.0556
0.1	1.0133	1.0133	1.0822	1.0822
0.2	0.9665	0.9665	1.0997	1.0997
0.3	0.9071	0.9071	1.0919	1.0919
0.4	0.8299	0.8299	1.0487	1.0487
0.5	0.7324	0.7324	0.9648	0.9648
0.6	0.6137	0.6137	0.8385	0.8385
0.7	0.4743	0.4743	0.6708	0.6708
0.8	0.3155	0.3155	0.4642	0.4642
0.9	0.1385	0.1385	0.2215	0.2215
1.0	-0.0556	-0.0556	-0.0556	-0.0556

Table 4. Comparison of various values of η for rotation profile.

η	RK-4 *@Re=5*	Present Work *@Re=5*	RK-4 *@Re=10*	Present Work *@Re=10*
0.0	0.0000	0.0000	0.0000	0.0000
0.1	0.0674	0.0674	0.0674	0.0674
0.2	0.0899	0.0899	0.0899	0.0899
0.3	0.0787	0.0787	0.0787	0.0787
0.4	0.0450	0.0450	0.0450	0.0450
0.5	0.0000	0.0000	0.0000	0.0000
0.6	-0.0450	-0.0450	-0.0450	-0.0450
0.7	-0.0787	-0.0787	-0.0787	-0.0787
0.8	-0.0899	-0.0899	-0.0899	-0.0899
0.9	-0.0674	-0.0674	-0.0674	-0.0674
1.0	0.0000	0.0000	0.0000	0.0000

4- Conclusion

This paper investigates the micro polar fluid flow through penetrable walls under slip flow and thermal jump conditions. The rheological parameters of thermal exchange and mass transport of the micro polar fluid are studied considering transport conditions. The mechanics of the fluid are described by coupled, highly successive, nonlinear system of higher order partial differentials transformed into ordinary differentials. These are analyzed by adopting the Homotopy perturbation method of analysis. Obtained results from the analysis were utilized in the study of the slip and thermal jump effect on micropolar fluid transport. It can be deduced from the study that:

i. Quantitative increase of nanoparticles concentration from $1-4\%$ enhances thermal transfer, which effect is significant towards the lower plate.

ii. Radiation increase reveals higher heat transfer while Reynolds parameter shows reducing heat transfer.

iii. Shear stress is enhanced at the boundary due to a rise in fluid vortex viscosity.

iv. Heat transfer across the transport medium improves due to radiation enhancement of rotating molecules on thermal exchange.

The results obtained were compared to Runge Kutta Fehlberg's numerical method for a simplified case which proved satisfactory. The study proves useful in scientific applications including tribology, and arterial blood flow amongst other relevant applications.

References

[1] A.C. Eringen, Theory of Micropolar fluids, Journal of mathematical Mechanics, 16 (1966) 1-18.

[2] M.D. Aurangzaib, S. Uddin, K. Bhattacharyya, S. Shafie, Micropolar fluid flow and heat transfer over an exponentially permeable shrinking sheet, Propulsion and Power Research, 5(4) (2016) 310-317.

[3] R.N. Bank, G.C. Dash, Chemical reaction effect on peristaltic motion of micropolar fluid through a porous medium with heat absorption the presence of magnetic field, Advances in Applied Science Research, 6 (2015)

20-34.

[4] M, Sheikholeslami, M. Hatami, D.D. Ganji, Micropolar fluid flow and heat transfer in a permeable channel using analytical method, Journal of Molecular Liquids, 194 (2014) 30-36.

[5] K.S. Mekheir, S.M. Mohammed, Interaction of pulsatile flow on peristaltic motion of magneto micropolar fluid through porous medium in a flexible channel: Blood flow model, International Journal Pure and Applied Mathematics, 94 (2014) 323-339.

[6] K. Ahmad, A. Ishak, R. Nazar, Micropolar fluid flow and heat transfer over a nonlinear stretching plate with viscous dissipation, Mathematical Problems in Engineering, 13 (2013) Article ID: 257161.

[7] S. Deo, D.K. Maurya, A.N. Filippo, Influence of magnetic field on micropolar fluid flow in a cylindrical tube enclosing an impermeable core coated with porous layer, Colloid Journal , 82 (2020) 649-660.

[8] M. Trkyilmazoglu, Mixed convection flow of magnetohydramic micropolar due to a porous heater / heated deformable plate: exact solution, International Journal Heat Mass Transfer, 106 (2017) 127-134.

[9] A.T. Akinshilo, Flow and heat transfer of nanofluid with injection through an expanding or contracting porous channel under magnetic force field, Engineering Science and Technology, an International Journal, 21 (2018) 486-494.

[10] L.I. Lund, Z. Omar, I. Khan, J. Raza, E.M. Sharif, A.H. Seikh, Magneto hydrodynamic (MHD) flow of micropolar fluid with effects of viscous dissipation and joule heating over an exponential shrinking sheet: Triple solution and stability analysis, Symmetry, 12(142) (2015) 1-16

[11] S. Ahmad, M. Ashraf, K. Ali, K.S. Nisar, Computational analysis of heat transfer and mass transfer in a micropolar fluid flow through a porous medium between permeable walls, International Journal of Nonlinear Sciences and Numerical Simulation, 52 (4) (2020) 101-113

[12] R.A. Damseh, M.Q. Al-Odat, A.J. Chamkha, B.A. Shannak, Combined effect of heat generation or absorption and first-order chemical reaction on micropolar fluid flows over a uniformly stretched permeable surface: The full analytical solution, International Journal of Thermal Science, 48 (8) (2009) 1658-1663.

[13] M. Alizadeh, A.S. Dogonchi, D.D. Ganji, Micropolar nanofluid flow and heat transfer between penetrable walls by the presence of thermal radiation and magnetic field, Case Studies in Thermal Engineering, 12 (2018) 319-322.

[14] M.M. Rahman, I.A. Eltayeb, S. Mohammad, M. Rahaman, Thermo-micropolar fluid flow along a vertical permeable plate with uniform surface heat flux in the presence of heat generation, Thermal Science, 13(1) (2009) 23-26.

[15] A.T. Akinshilo, Investigation of nanofluid conveying porous medium through non-parallel plates using the Akbari Ganji method, Physica Scripta 95 (12) (2019) 1-11 .

[16] T. Hayat, T. Nasir, M.I. Khan, A. Alsaedi, Non-Darcy flow of water based single (SWCNTS) and multiple (MWCNTS) walls carbon nanotubes with multiple slip condition due to rotating disk, Results in Physics, 9 (2019) 390-399.

[17] S.R. Yan, R. Kalbasi, Q. Nguyen, A. Karimipour, Sensitivity of adhesive and cohesive intermolecular forces to the incorporation of MWCNTs into liquid paraffin: Experimental study and modelling of surface tension, Journal of Molecular Liquids, 310 (2020) 113235.

[18] Z. Tian, S. Rostamis, T. Taherialekouhi, A. Karimipour, A. Moradikazerouni, H. Yarmand, N.W.B.M. Zulkifli, Prediction of rheological behavior of a new hybrid nanofluid consists of copper oxide and multi walled carbon nanotubes suspended in a mixture of water and ethylene glycol using curve fitting on experimental data, Physica A: Statistical Mechanics and Its Applications, 549 (2020) 124101.

[19] B. Sharifzadeh, R. Kalbasi, M. Jahangiri, D. Toghraie, A. Karimipour, Computer modelling of pulsatie blood flow in elastic artery using a software program for application in biomedical engineering, Computer Methods and Programs in Biomedicine, 192 (2020) 105442.

[20] M. Farzinpour, D. Toghraie, B. Mehmandoust, F. Aghadavoudi, A. Karimipour, Molecular dynamics study of barrier effects on ferro-nanofluid flow in the presence of constant and time dependent external magnetic field, Journal of Molecular Liquids, 308 (2020) 113152.

[21] S.R. Yan, R. Kalbasi, Q. Nguyen, A. Karimpour, Rheological behavior of hybrid MWCNTs-TiO2/EG nanofluid: A comprehensive modelling and experimental study, 306 (2020) 112937.

[22] A. Zakari, M. Ghalambaz, A.J. Chamkha, D.D. Rossi, Theoretical analysis of natural convection boundary layer heat and mass transfer of nanofluids: effects of size, shape and type of nanoparticles, type of base fluid and working temperature, Advanced Powder Technology, 26(3) (2015) 935-946

[23] A.J. Chamkha, A. Al-Mudhaf, Unsteady heat and mass transfer from a rotating vertical cone with a magnetic field and heat generation or absorption effects, International Journal of Thermal Science, 44(3) (2005) 267-276

[24] S.H. Reddy, M.C. Raju, E.K. Reddy, Magneto convective flow of a non-Newtonian fluid through non-homogeneous porous medium past a vertical porous plate with variable suction, Journal of Applied Mathematics and Physics 4 (2016) 233-248.

[25] M. Naravhani, Unsteady free convection flow past a semi-infinite vertical plate with constant heat flux in water based nanofluids, IOP Conference Series: Materials Science and Engineering, 15, (2018) 81-94.

[26] R. Subba, R., Gorla, A.J. Chamkha, Natural convective boundary layer flow over a nonisothermal vertical plate embedded in a porous medium saturated with a nanofluid,

Nanoscale and Microscale Thermophysical Engineering, 15 (2) (2010) 81-94.

[27] A.W. Xiao, H.J. Lee, I. Capone, A. Robertson, T. Wi, J. Fawdon, S. Wheeler, H.W. Lee, N. Grobert, M. Pasta, Understanding the conversion mechanism and performance of monodisperse FeF2 nanocrystal cathode, Nature Materials , 19 (2020) 644-654.

[28] D.J. Lewis, L.Z. Zomberg, D.J.D. Carter, R.J. Macfarlane, Single crystal winter bottom constructions of nanoparticles super lattices , Nature Material, 19 (7) (2020) 719-724.

[29] H. Dessie, N. Kishan, MHD effects on heat transfer over stretching sheet embedded in porous medium with variable viscosity, viscous dissipation and heat source/ sink, Ain Shams Engineering Journal , 5 (3) (2014) 967-977.

[30] S.M. Ibrahim, Radiation effects on mass transfer flow through a highly porous medium with heat generation and chemical reaction, International Scholarly Research Notices,13 (2013) Article ID 765408.

[31] B. Souyeh, M.G. Reddy, P. Sreenivasulu, T. Poornima, M. Rahimi-Gorji, I.M. Alarifi, Comparative analysis on non-linear radiative heat transfer on MHD Casson nanofluid past a thin needle, Journal of Molecular Liquids, 284 (2019) 163-174.

[32] A.T. Akinshilo, A.G. Davodi, A. Ilegbusi, M.G. Sobamowo, Thermal analysis of radiating film flow of sodium alginate using MWCNT nanoparticles, Journal of Applied and Computational Mechanics 8 (1) (2020) 219-231.

[33] A. Pantokratoras, T. Fang, Sakiadis flow with nonlinear Rosseland thermal radiation, Physica Scripta, 87 (1) (2013) 015703.

[34] H. Khan, M. Haneef, Z. Shah, S. Muhammad, S. Islam, W. Khan, The combined magneto hydrodynamic and electric field effect on unsteady Maxwell nanofluid flow over a stretching surface under the influence of variable heat and thermal radiation, Applied Science, 8 (2) (2018) 160

[35] B. Mahanthesh, B.J. Gireesha, I.L. Animasaun, Exploration of non-linear thermal radiation and suspended nanoparticles effects on mixed convection boundary layer flow on nano liquids on a melting vertical surface , Journal of Nanofluids 7 (5) (2018) 833-843.

[36] M. Mustafa, A. Mushtaq, T. Hayat, B. Ahmad, Nonlinear radiation heat transfer effects in the natural convective boundary layer flow of nanofluid past a vertical plate: a numerical study, PlosOne, 9(9) (2014) e103946.

[37] L. Dianchen, M. Ramzan, N.U. Huda, J.D. Chung, U. Farooq, Nonlinear radiation effect on MHD Carreau nanofluid over a radially stretching surface , Science Reports, 8 (2018) 3709.

[38] J.V. Ramana Reddy, V. Sugunamma, N. Sandeep, Thermophoresis and Brownian motion effects on unsteady MHD nanofluid flow over a slandering surface with slip effects, Alexandria Engineering Journal, 57 (4) (2017) 2465-2473.

[39] M.K. Nayak, F. Mabood, O.D. Makinde, Heat transfer and buoyancy-driven convective MHD flow of nanofluids impinging over a thin needle moving in a parallel stream influenced by Prandtl number, Heat Transfer—Asian Research,49 (2) (2019) 1–18.

[40] S.N.A. Salleh, N. Bachok, N. Md. Arifin, F. Md. Ali, I. Pop, Stability analysis of mixed convection flow towards moving a thin needle in nanofluid, Applied Science, 8(6) (2018) 842.

[41] P. Mohan Khrishna, R. Prakash Sharma, N. Sandeep, Boundary layer analysis of persistent moving horizontal needle in Blasius and Sakiadis magnetohydrodynamic radiative nanofluid flow, Nuclear Engineering Technology, 49 (8) (2017) 1654-1659.

[42] C. Sulochana, G.P. Ashwinkumar, N. Sandeep, Joule heating effect on a continuously moving thin needle in MHD Sakiadis flow with thermophoresis and Brownian moment , The European Physical Journal Plus, 132 (2017) 387.

[43] O. Pourmehran, M.M. Sarafraz, M. Rahimi-Gorji, D.D. Ganji, Rheological behaviour of various metal-based nano-fluids between rotating discs: a new insight Journal of the Taiwan Institute of Chemical Engineers, 18 (2018) Article ID:644800.

[44] H. Mirgolbabaee, S.T. Ledari, M. Sheikholeslami, D.D. Ganji, Semi-analytical investigation of momentum and heat transfer of a non-Newtonian fluid flow for specific turbine cooling application using AGM, International Applied Computational Mathematics, 3 (2017) S1463-S1475.

[45] A.T Akinshilo, A.O. Ilegbusi, H. Ali, A. Surajo. Heat transfer analysis of nanofluid flow with porous medium through Jeffery Hamel diverging/converging channel, Journal of Applied and Computational Mechanics, 6(3) (2020) 433-444.

[46] A.T. Akinshilo, Thermal performance evaluation of MHD nanofluid transport through a rotating system undergoing uniform injection/suction with heat generation, Bionanoscience, 9 (3) (2019) 740-748.

[47] F. Mabood, A.T. Akinshilo, Stability analysis and heat transfer of hybrid Cu-Al2O3/H2O nanofluids transport over a stretching surface, International Communications in Heat and Mass Transfer, 123 (2021) 105215.

[48] S. Shen, Application of He's variational iteration method to the fifth order boundary value problems, Journal of Physics Conference Series, 96 (2008) 012185.

[49] G. Domairry, Z. Ziabakhsh, H. Doumiri, G. Modil Habib, Approximate solution of non-Newtonian viscoelastic fluid flow on a turbine disc for cooling purpose by using Adomian decomposition method, Meccanica, 98 (2013) 4889-4909.

[50] A.S. Dogonchi, M. Alizadeh, D.D. Ganji, Investigation of MHD GO-water nanofluid flow and heat transfer in a porous channel in the presence of thermal radiation effect, Advanced Powder Technology, 28 (7) (2017)

1815-1825 .

[51] A.S. Dogonchi, D.D. Ganji, Investigation of MHD nanofluid flow and heat transfer in a stretching /shrinking convergent/divergent channel considering thermal radiation, Journal of Molecular Liquid, 220 (2016) 592-603.

HOW TO CITE THIS ARTICLE

A. T. Akinshilo, M. G. Sobamowo, A. Adingwupu, Evaluation of Micropolar Fluid Transport through Penetrable Medium: Effect of Flow and Thermal Slip , AUT J. Mech Eng., 6 (3) (2022) 427-442.

DOI: 10.22060/ajme.2022.20632.6012